INTERNATIONAL COUNCIL FOR SCIENCE

INTERGOVERNMENTAL OCEANOGRAPHIC COMMISSION

WORLD METEOROLOGICAL ORGANIZATION

WORLD CLIMATE RESEARCH PROGRAMME

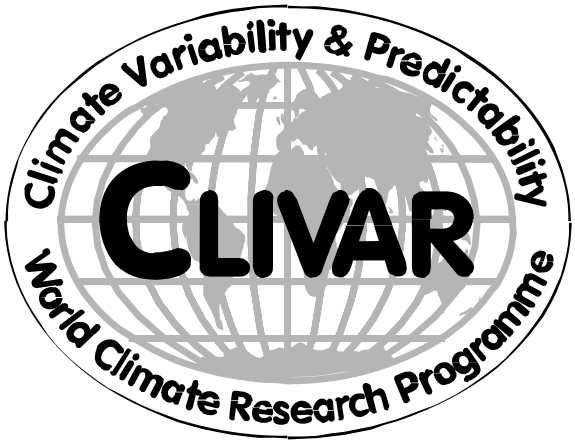

Sampling Physical Ocean Field in SCRP CMIP5 Simulations: CLIVAR Working Group on Ocean Model Development (WGOMD) Committee on CMIP5 Ocean Model Output

February 2009

ICPO Publication Series No.137

WCRP Informal Report No. 3/2009

Arctic Circle, is readily approximated as the $\hat{\mathbf{y}}$-ward transport, as defined along the model's native grid lines. These streamfunctions are sensibly compared between models with varying grid choices, again since regions where the grid lines are most highly distorted from the sphere are precisely those regions where the flow is very weak and thus of less interest for scientific purposes.

- Transport in regions north of the Arctic Circle is very weak relative to transport in the south, and poorly sampled from observations. Hence, its diagnosis is of secondary concern for comparison to observations.
- The overturning streamfunction is not a directly observed field. Instead, it is partialy inferred through selected transport measurements at very few ocean sections. To constrain the recording of the simulated streamfunction to be oriented precisely along a line parallel to geographical longitude is not warranted for reasons of comparing to observations.

A general expression for the ocean mass transport overturning streamfunction is given by

$$\Psi(y, s, t) = -\int_{x_a}^{x_b} \mathrm{d}x \int_{-H}^{z(s)} \rho \, v^{\text{total}} \, \mathrm{d}z, \tag{4.17}$$

where v^{total} is the native grid approximation to the poleward transport arising from the resolved velocity component, plus all SGS processes contributing to mass transport. Note that the zonal integral is computed along surfaces of constant s, where s is either a geopotential/pressure surface, or a potential density surface. That is, we recommend that the following versions of the overturning streamfunction be archived at monthly time averages in the CMIP5 repository, with results for the Atlantic-Arctic, Indian-Pacific, and Global Oceans:

- **poleward-depth overturning streamfunction** and **$\hat{\mathbf{y}}$-ward-depth overturning streamfunction**: The depth $z(s)$ corresponds to either the depth of a geopotential or the depth of a pressure surface, depending on whether the model is Boussinesq or non-Boussinesq, respectively.
- **poleward-density overturning streamfunction** and **$\hat{\mathbf{y}}$-ward-density overturning streamfunction**: The depth $z(s)$ corresponds to the depth of a predefined set of σ_{2000} isopycnals, with the definition of these isopycnals at the modeler's discretion. This field presents complementary information relative to the $\hat{\mathbf{y}}$-ward-depth overturning streamfunction, and is very useful particularly for diagnosing water mass transformation processes.[25]
- Consistent with the discussion in Section 3.1.1, it is critical that the time average of the streamfunction be accumulated using each model time step, in order to avoid problems with aliasing and problems ignoring correlations.

4.3.6 Poleward and ŷ-ward overturning streamfunction from SGS transport (2)

- ocean_meridional_overturning_mass_streamfunction_due_to_bolus_advection
- ocean_y_overturning_mass_streamfunction_due_to_bolus_advection

We follow the same philosophy as above for diagnosing the poleward and $\hat{\mathbf{y}}$-ward overturning streamfunction arising just from SGS transport. There are two notable SGS methods whose overturning we recommend archiving: Gent et al. (1995) and the newer mixed layer transport scheme from Fox-Kemper et al. (2008). Other schemes may also be included, so long as they impact on the overturning mass streamfunction. That is, both the Gent et al. (1995) and Fox-Kemper et al. (2008) introduce a new streamfunction, with the name "bolus" generically ascribed to this streamfunction based on historical reasons. Note that since the Fox-Kemper et al. (2008) scheme applies only in the mixed layer, only its poleward-depth and $\hat{\mathbf{y}}$-depth version is relevant. For the Gent et al. (1995) streamfunction, it is useful to map this in both depth and density space.[26]

4.3.7 Vertically integrated heat transport from all processes (1)

- northward_ocean_heat_transport
- ocean_heat_x_transport
- ocean_heat_y_transport

There are many processes in the ocean that affect the heat transport: resolved advective transport, diffusion, skew diffusion, overflow parameterizations, etc. In the analysis of ocean model simulations, it is very useful to have a measure of each component of the heat transport. We suggest the vertically integrated $\hat{\mathbf{x}}$-ward and $\hat{\mathbf{y}}$-ward heat transport from all processes, archived as monthly means for the Atlantic-Arctic, Indian-Pacific, and World Ocean, and maintained on the model's native grid. In addition, following from the approach taken for the meridional overturning streamfunction, each ocean model using non-spherical coordinate horizontal grids should compute the poleward heat transport in each of the basins, approximated using the model's native grid fields without remapping. The approximated poleward transport will generally consist of transports crossing a "zig-zag" path. The resulting poleward heat transport should be reported as a function of latitude, with latitudinal resolution comparable to the model's native grid resolution. This recommendation follows that from WGCM (2007), with the method to calculate the transports now explicitly specified.

4.3.8 Vertically integrated heat transport from SGS processes (2)

- northward_ocean_heat_transport_due_to_bolus_advection
- northward_ocean_heat_transport_due_to_diffusion
- ocean_heat_x_transport_due_to_bolus_advection
- ocean_heat_x_transport_due_to_diffusion
- ocean_heat_y_transport_due_to_bolus_advection
- ocean_heat_y_transport_due_to_diffusion

In support of understanding the importance of various SGS physical parameterizations, we recommend that separate heat transports should be archived as follows.

- Parameterized SGS advection, as from Gent and McWilliams (1990); Gent et al. (1995) and the scheme from Fox-Kemper et al. (2008), should be included in the fields "due_to_bolus_advection", even if the implementation of the schemes appears as a skew diffusion. In addition, include the effects from neutral/isopycnal diffusion (see comments below).
- Any remaining SGS processes, such as overflow parameterizations, etc., should be included in the "due to diffusion" fields.

These standard names are imprecise. They are largely based on historical reasons that are somewhat obsolete. The main reason to combine the SGS advection processes, such as Gent et al. (1995), with neutral diffusion is that many model implementations follow the approach of Griffies (1998). Here, neutral diffusion and Gent et al. (1995) are combined into a single operator, in which case the "bolus advection" from Gent et al. (1995) is transformed to a skew diffusion. The combined neutral diffusion and skew diffusion is thus better considered a single "neutral physics" operator, with it impractical algorithmically to then split this operator into two pieces for purposes of diagnostics. We therefore request models to include all of these "neutral physics" processes within the fields "due_to_bolus", even if the models do not implement Gent et al. (1995) according to a skew diffusion approach. Information regarding these details should be clearly stated in the meta-information for the fields.

We recommend archiving these heat transports both on the model's native grid, as well as the poleward transport approximated using the a "zig-zag" path method discussed previously. The components should be archived as monthly means for the Atlantic-Arctic, Indian-Pacific, and World Ocean. The transports should be reported as a function of latitude, with the latitudinal spacing comparable to the model's native grid spacing.

4.3.9 Vertically integrated heat & salt transport from gyre and overturning components (1)

- northward_ocean_heat_transport_due_to_gyre
- northward_ocean_heat_transport_due_to_overturning
- northward_ocean_salt_transport_due_to_gyre
- northward_ocean_salt_transport_due_to_overturning

The $\hat{\mathbf{y}}$-ward advective transport of a tracer within a particular ocean basin is given by the integral

$$\mathcal{H}^{\hat{\mathbf{y}}}(y,t) = \int_{x_1}^{x_2} \mathrm{d}x \int_{-H}^{\eta} \mathrm{d}z\, \rho\, C\, v, \tag{4.18}$$

where C is the tracer concentration, $z = -H(x, y)$ is the ocean bottom, $z = \eta(x, y, t)$ is the ocean surface, and x_1 and x_2 are the boundaries of the basin or global ocean. It is useful for some analysis to decompose the transport (4.18) into "gyre" and "overturning" components, with these terms defined in the following endnote.[27] We recommend that the monthly means for the components to heat and salt transport, partitioned according to Atlantic-Arctic, Indian-Pacific, and Global Oceans, be archived in the following manner:

- For all processes affecting the tracer, including resolved and SGS processes.
- For just the resolved scale flow.

We recommend archiving these transports both on the model's just as the poleward transport approximated using the a "zig-zag" path method discussed previously. The components should be archived as monthly means for the Atlantic-Arctic, Indian-Pacific, and World Ocean. The transports should be reported as a function of latitude, with the latitudinal spacing comparable to the model's native grid spacing.

4.4 Integrated mass transports

- sea_water_transport_across_line

1. barents_opening
2. bering_strait
3. canadian_archipelago
4. denmark_strait
5. drake_passage
6. english_channel
7. equatorial_undercurrent
8. faroe_scotland_channel
9. florida_bahamas
10. fram_strait
11. iceland_faroe_channel
12. indonesian_throughflow
13. mozambique_channel
14. taiwan_and_luzon_straits
15. windward_passage

There are a number of climatologically important straits, throughflows, and current systems whose integrated mass transport is measured observationally (though some have wide uncertainties). These mass transports provide a useful means to characterize the simulation. Transports were not archived in CMIP3, thus necessitating a diagnostic calculation from the archived velocity field and/or the barotropic streamfunction. Such diagnoses, however, can be subject to uncertainty, especially for models with complex horizontal and vertical grids. It is thus more direct and accurate to have these transports computed by each participating model group, and archived as part of CMIP5. Table 2.4 provides a list of recommended transports for CMIP5. Each geographical region has an associated string valued coordinate given by the name.

We make the following recommendations regarding the recording of integrated mass transports.

- In the following, we note the approximate geographical longitude and latitude coordinates of the straits and currents. Given considerations of model grid resolution and grid orientation, precise values for the coordinates may differ for any particular model. *In general, we recommend computing the simulated transport where the strait is narrowest and shallowest in the model configuration, and where the model grid is closely aligned with the section*.
- For most ocean model grids, the requested transports can be diagnosed by aligning the section along a model grid axis. In this case, it is straightforward to assign a positive sign to transports going in a pseudo-north or pseudo-east direction, and negative signs for the opposite direction. We use the term *pseudo* here as it refers to an orientation according to the model grid lines, which in general may not agree with geographical longitude and latitude lines. In general, the sign convention chosen for the recorded transport should be clearly indicated in the metadata information for the transport field.

- Some models may have a strait artificially closed, due to inadequate grid resolution. In this case, a zero transport should be recorded for this strait.
- We present references to observational estimates for the mass transports. These references will be kept updated on the WGOMD web page `www.clivar.org/organization/wgomd/reos/reos.php` as new results become available. Notably, there are some straits with large uncertainties. Even so, recording transport results from the various models will present the community with a valuable means to characterize the model flow fields.
- Some of the following transports are defined in accordance with the Global Ocean Data Assimilation Experiment (GODAE), as detailed in the report by the MERSEA project (MERCATOR, 2006).

The following provides details for the various regions where integrated mass transport is requested for CMIP5.

1. Barents Opening: The Barents Opening separates Spitsbergen from Norway. Vertically integrated transport through the Barents Opening occurs geographically roughly between the points

   - Barents opening = $(16.8^\circ E, 76.5^\circ N)$ to $(19.2^\circ E, 70.2^\circ N)$.

   Observational estimates range from 1.5-2.0 Sv northwards, with large variability, thus necessitating longer time series to get a zero order estimate.

2. Bering Strait: The Bering Strait separates Alaska from Siberia. Vertically integrated transport through the Bering Strait provides the only exchange between Pacific and Arctic waters. It is defined geographically from

   - Bering Strait = $(171^\circ W, 66.2^\circ N)$ to $(166^\circ W, 65^\circ N)$.

   An observational estimate from Roach et al. (1995) is 0.8Sv northward from the Pacific into the Arctic Ocean.

3. Canadian Archipelago: The Canadian Archipelago refers to the wide range of Arctic islands in northern Canada. The transport through these islands connects waters of the open Arctic to the North Atlantic through the Davis Strait and into the Labrador Sea. Vertically integrated transport through the Canadian Archipelego can be defined according to the following geographic region

   - Canadian Archipelego = $(128.2^\circ W, 70.6^\circ N)$ to $(59.3^\circ W, 82.1^\circ N)$.

   Observational estimates range from 0.7 to 2.0Sv southward (Sadler, 1976; Fissel et al., 1998; Melling, 2000).

4. Denmark Strait: The Denmark Strait separates Greenland from Iceland. Vertically integrated transport between Iceland and Greenland occurs over the following geographical region

   - Denmark Strait = $(37^\circ W, 66.1^\circ N)$ to $(22.5^\circ W, 66^\circ N)$.

   Observational estimates are 0.8Sv for the net northward transport (Osterhus et al., 2005) and 3Sv for the net southward transport (Olsen et al., 2008).

5. Drake Passage: The Drake Passage separates South America from Antarctica. It presents the narrowest constriction for the Antarctic Circumpolar Current. Vertically integrated transport in the Southern Ocean through the Drake Passage is determined by flow through the region

   - Drake Passage = $(68^\circ W, 54^\circ S)$ to $(60^\circ W, 64.7^\circ S)$.

   An observational estimate from Cunningham et al. (2003) is an eastward transport of 135Sv.

6. English Channel: The English Channel separates Britian from the European continent. Vertically integrated transport in the English Channel occurs geographically through the region

   - English Channel = $(1.5^\circ E, 51.1^\circ N$ to $(1.7^\circ E, 51.0^\circ N)$.

   Observational estimates from Otto et al. (1990) are roughly $0.1 - 0.2$Sv northward.

7. Equatorial Undercurrent: A commonly used region to measure transport in the equatorial undercurrent is given by the region

   - Equatorial Undercurrent = $(155^\circ W, 3^\circ S)$ to $(155^\circ W, 3^\circ N)$ over the depth range 0-350m.

   Observational estimates range between 24Sv-36Sv in an eastward direction (Lukas and Firing, 1984; Sloyan et al., 2003).

8. Faroe-Scotland Channel: The Faroe-Scotland Channel separates the Faroe Islands from Scotland. Vertically integrated transport between the Faroe Islands and Scotland occurs geographically through the region between

- Faroe-Scotland Channel = (6.9°W, 62°N) to (5°W, 58.7°N)

Observational estimates are 3.8Sv for the net northward transport (Osterhus et al., 2005) and 2.1Sv for the net southward transport (Olsen et al., 2008).

9. Florida-Bahamas Strait: Since 1982 cables have been used to measure the transport of the Florida Current between Florida and the Bahamas near 27N. We thus define this transport according to the following geographical locations

   - Florida-Bahamas Strait = (78.5°W, 26°N) to (80.5°W, 27°N).

   Observational estimates range from 29Sv-35Sv (Leaman et al., 1987). Updated information is available from AOML at `www.aoml.noaa.gov/phod/floridacurrent/`. See also Figure 2-6 from the MERSEA project (MERCATOR, 2006).

10. Fram Strait: The Fram Strait separates Spitsbergen from Greenland. Vertically integrated transport in the Fram Strait occurs geographically through the region

    - Fram Strait = (11.5°W, 81.3°N to (10.5°E, 79.6°N).

    Observational estimates from Schauer et al. (2004) are 4 ± 2Sv southwards.

11. Iceland Faroe Channel: The Iceland Faroe Channel separates Iceland from the Faroe Islands. Vertically integrated transport between Iceland and the Faroe Islands occurs geographically through the region between

    - Iceland-Faroe Channel = (13.6°W, 64.9°N) to (7.4°W, 62.2°N)

    Observational estimates are 3.8Sv for the net northward transport (Osterhus et al., 2005) and 1Sv for the net southward transport (Olsen et al., 2008).

12. Indonesian Throughflow: Vertically integrated transport through the Indonesian Archipelogo is defined approximately by

    - Indonesian Throughflow = (100°E, 6°S) to (140°E, 6°S).

    An observational estimate from Gordon et al. (2003) is roughly 10Sv from the Pacific to the Indian Oceans.

13. Mozambique Channel: The Mozambique Channel separates Madagascar from the African continent. Vertically integrated transport through the Mozambique channel separating Madagascar from Southeast Africa is defined approximately by

    - Mozambique Channel = (39°E, 16°S) to (45°E, 18°S).

14. Taiwan-Luzon Straits: We ask here for the vertically integrated transport giving the combined inflow to the South China Sea through the Taiwan and Luzon straits. The value from observations is positive when entering the South China Sea, and Yaremchuk et al. (2008) present a review of observed values.

15. Windward Passage: The Windward Passage lies between the easternmost region of Cuba and the northwest of Haiti, and is defined approximately by

    - Windward Passage = (75°W, 20.2°N) to (72.6°W, 19.7°N).

4.5 Boundary fluxes

The ocean is a forced-dissipative system, with forcing largely at its boundaries. To develop a mechanistic understanding of ocean simulations, it is critical to have a clear sampling of the many forcing fields. Some of the following fields can be found in other parts of the CMIP5 archive as part of the sea ice or atmosphere components. However, these fields are typically on grids distinct from the ocean model grid. Fluxes on grids distinct from the ocean make accurate budget analyses difficult to perform, and such was a major shortcoming of the CMIP3 archive (WGCM, 2007). For CMIP5, we wish to resolve this problem by requesting an archive of the precise boundary fluxes used to force the ocean model.

We offer the following general comments regarding the boundary flux fields. Details of the requested fluxes are given in the subsequent subsections.

- All fluxes (water mass, salt mass, heat, momentum) are normalized according to the horizontal area of the ocean model grid cell. In some cases (e.g., rainfall), the flux computation requires integrating the rainfall over the ice-free sea (to get a mass per time of rainfall) and then dividing by the ocean grid cell area (to get mass per time per area). For these fluxes, according to the CF metadata conventions, the cell_methods attribute for the fields should read

  – area: mean where ice_free_sea over all_area_types.

  In other cases (e.g., melting sea ice) the flux computation requires integrating the sea ice melt over the sea ice covered portion of the ocean grid cell, and then dividing by the ocean grid cell area. For these fluxes, according to the CF metadata conventions, the cell_methods attribute for the fields should read

  – area: mean where sea_ice over all_area_types.

- Multiplication of a boundary flux by the ocean model grid cell area allows for the mass, heat, or momentum passed to the ocean, per time, to be computed.
- Many climate models place boundary fluxes just at the ocean surface. However, more general couplings are being considered (e.g., penetrative shortwave heating; sea ice models that interact with more than the surface ocean cell). To allow for such generality, we ask that those fluxes that are three-dimensional be archived with their full three dimensional structure.
- To remphasize a point raised throughout this document, the wind stresses and ice stresses should be reported on the ocean model native grid, with no remapping or rotation.
- The term "flux correction" in Tables 2.5, 2.6, 2.7, and 2.8 refers to the imposition of a prescribed flux that has at most a monthly variability (sometimes only an annual mean adjustment is imposed). Flux corrections (also called flux adjustments) have no interannual variability. They are added to some climate models for the purpose of reducing model drift. However, flux corrections are becoming less common as models are improved, in which case they are zero (see, for example, Section 8.4.2 of McAvaney et al., 2001).
- Some ocean models do not allow for the passage of water mass across the liquid ocean boundaries. Virtual salt fluxes are instead formulated to parameterize the effects of changes in salinity on the density field (Huang, 1993; Griffies et al., 2001). The models that use virtual fluxes do not have a physically correct water cycle, as there is zero exchange of water between the ocean and other components of the climate system. Correspondingly, they do not have a physically correct salt budget, since the real ocean system has a trivial net flux of salt across the ocean surface boundary, contrasting with the nontrivial virtual salt fluxes.
- The passage of water across an ocean boundary (via precipitation, evaporation, and runoff) corresponds to a transfer of tracer across the boundary, since the water generally carries tracer (e.g., carbon, heat). Heat from this water transport (relative to $0^{\circ}C$) is requested in the Table 2.7. Notably, this heat transport is distinct from the heat transport associated with phase changes. Instead, the heat transport is due solely to the nontrivial heat present in water that moves between the ocean and other components of the climate system. Models that artificially preclude water to cross the ocean boundary (e.g., rigid lid models, or models with a virtual tracer flux) have zero contributions to these transport induced heat fluxes.

  For precipitation and evaporation, the heat flux associated with water transport across the ocean boundaries generally provides a global net cooling of the ocean, since evaporation transfers water away from the ocean at a temperature typically higher than precipitation adds water. In a steady state, this net heat loss is compensated by ocean heat transport, and the ocean heat transport is in turn balanced by atmospheric heat transport. However, most atmospheric models do not carry the temperature of its moisture field, thus precluding the atmospheric component in a climate model from representing the heat transport. There is a resulting non-conservative heat budget in the simulated climate system.

  The size of the atmospheric heat transport associated with the temperature of its moisture field is small relative to the atmospheric heat fluxes associated with phase changes of water in the atmosphere. It is the dominance of heating associated with phase change that has motivated atmospheric modelers to ignore the temperature of its moisture field. In contrast, ocean water must be tagged with its temperature field in order to simulate the ocean fluid, providing a generally nonzero heat associated with water that passes across ocean boundaries. The reader is referred to Section 3 of the coupled model paper from Delworth et al. (2006), where an estimate for the heat flux is given. Section D.2 of the ocean model comparison paper by Griffies et al. (2009) also provides a discussion of this heat flux.

4.5.1 Boundary fluxes of water mass

- rainfall_flux
- snowfall_flux
- water_evaporation_flux
- water_flux_into_sea_water_from_rivers
- water_flux_into_sea_water_from_icebergs
- water_flux_into_sea_water_due_to_sea_ice_thermodynamics
- water_flux_into_sea_water
- water_flux_into_sea_water_without_flux_correction
- water_flux_correction

These fluxes (Table 2.5) aim to present the analyst with sufficient information to perform a water mass budget on the liquid ocean. Models that employ a virtual salt flux, and so do not allow for the transfer of water mass across the liquid ocean boundary, will report zero for each of these fields. The following presents some general comments.

- Liquid runoff is defined as liquid water that enters the ocean from land, such as through rainwater in rivers, or snow and ice meltwater in rivers. It may also incorporate melt water from sea ice and icebergs.
- An iceberg model exports a certain amount of calved land ice away from the coasts. It is thus important to record where the icebergs melt (horizontal position and depth), hence the suggestion to include iceberg melt (Table 2.5).

We now present detailed comments about each of the fields. As discussed in the first bulleted item at the beginning of Section 4.5, the fluxes, which may be defined only over a portion of each ocean grid cell, are normalized by the full area of each ocean grid cell. As a result, the product of the ocean horizontal area and the flux will render the full mass entering or leaving the liquid ocean.

- rainfall_flux: The mass flux of liquid precipitation from the atmosphere entering the ice-free portion of an ocean grid cell.
- snowfall_flux: The mass flux of frozen precipitation from the atmosphere entering the ice-free portion of an ocean grid cell.
- water_evaporation_flux: This is a flux that is positive for water leaving the liquid ocean. It measures the rate at which water vapor leaves the liquid ocean and enters the atmosphere, through the ice-free portion of an ocean grid cell.
- water_flux_into_sea_water_from_rivers: This field measures the mass of liquid water runoff entering the ocean from land-surface boundaries.
- water_flux_into_sea_water_from_icebergs: The solid mass that enters the ocean from land-ocean boundaries will eventually melt in the ocean. This melt may occur just at the ocean-land boundary, be distributed seawards by a spreading scheme, or participate in the transport via icebergs. It is this melt that is requested.
- water_flux_into_sea_water_due_to_sea_ice_thermodynamics: This is the contribution to liquid ocean mass due to the melt (positive flux) or freezing (negative flux) of sea ice.
- water_flux_into_sea_water: This is the net flux of liquid water entering the liquid ocean.
- water_flux_correction: This field stores the mass flux due to flux corrections.
- water_flux_into_sea_water_without_flux_correction: This field stores the mass flux due to physical processes absent the flux corrections.

4.5.2 Boundary fluxes of salt

- virtual_salt_flux_into_sea_water_due_to_rainfall
- virtual_salt_flux_into_sea_water_due_to_evaporation
- virtual_salt_flux_into_sea_water_from_rivers
- virtual_salt_flux_into_sea_water_due_to_sea_ice_thermodynamics
- virtual_salt_flux_correction

- virtual_salt_flux_into_sea_water
- downward_sea_ice_basal_salt_flux
- salt_flux_into_sea_water_from_rivers

These fluxes (Table 2.6) aim to present the analyst with sufficient information to perform a salt budget on the liquid ocean. The following presents some details about the fields. Note that for models using real water fluxes, the virtual salt flux fields will all be zero.

- virtual_salt_flux_into_sea_water_due_to_rainfall: This field measures the virtual salt flux associated with liquid precipitation.
- virtual_salt_flux_into_sea_water_due_to_evaporation: This field measures the virtual salt flux associated with the evaporation of liquid water.
- virtual_salt_flux_into_sea_water_from_rivers: This field measures the virtual salt flux associated with the liquid runoff from land processes.
- virtual_salt_flux_into_sea_water_due_to_sea_ice_thermodynamics: This field measures the virtual salt flux associated with the melting or freezing of sea ice.
- virtual_salt_flux_correction: This field measures the virtual salt flux arising from a salt flux correction.
- virtual_salt_flux_into_sea_water: This field measures the total virtual salt flux entering the ocean.
- Salt transport from sea-ice to the ocean is measured in the field downward_sea_ice_basal_salt_flux.
- Rivers may contain a nonzero salinity, in which case salt_flux_into_sea_water_from_rivers will be zero.

4.5.3 Boundary fluxes of heat

- upward_geothermal_heat_flux_at_sea_floor
- temperature_flux_due_to_rainfall_expressed_as_heat_flux_into_sea_water
- temperature_flux_due_to_evaporation_expressed_as_heat_flux_out_of_sea_water
- temperature_flux_due_to_runoff_expressed_as_heat_flux_into_sea_water
- heat_flux_into_sea_water_due_to_snow_thermodynamics
- heat_flux_into_sea_water_due_to_sea_ice_thermodynamics
- heat_flux_into_sea_water_due_to_iceberg_thermodynamics
- surface_net_downward_longwave_flux
- surface_downward_latent_heat_flux
- surface_downward_sensible_heat_flux
- surface_net_downward_shortwave_flux
- downwelling_shortwave_flux_in_sea_water
- heat_flux_correction

These fluxes (Table 2.7) aim to present the analyst with sufficient information to perform a heat budget on the liquid ocean. The following presents some details about the fields.

- upward_geothermal_heat_flux_at_sea_floor: Some ocean model components planned for CMIP5 employ geothermal heating through the ocean model's bottom surface. This heating is typically unchanging over the course of climate simulations, but there may be some efforts to allow for time dependence of the geothermal heating, in which case the monthly heat flux should be archived. It is assumed that models considering a geothermal heating will inject this heating at the sea-floor.
- temperature_flux_due_to_rainfall_expressed_as_heat_flux_into_sea_water: This field measures the heat carried by the transfer of rainfall into the liquid ocean, with the heat computed with respect to $0°C$. This heat is computed as

$$\text{rainfall heat } (\text{W/m}^2) = Q_{\text{rain}}\, C_p\, T_{\text{rain}}, \tag{4.19}$$

  where Q_{rain} is the rainfall mass flux in kg/(m^2 sec), C_p is the rainfall heat capacity, and T_{rain} is the temperature of rainfall in degrees Celsius. Most climate models choose the rainfall temperature to equal the ocean sea surface

temperature. The reason for this assumption is that atmsospheric models tend not to carry the temperature of their moisture field. But this assumption need not be applied for more complete atmospheric models.

For models employing a virtual tracer flux, in which there is no mass or volume transport of water across the ocean surface, the field temperature_flux_due_to_rainfall_expressed_as_heat_flux_into_sea_water is zero.

Note that since we measure this heat flux with respect to $0°C$, there is no need to record an analogous heat flux due to snowfall, if we assume the snow enters the ocean at $0°C$.

- temperature_flux_due_to_evaporation_expressed_as_heat_flux_out_of_sea_water: This field measures the heat carried by the transfer of water away from the liquid ocean through the process of evaporation. This heat is distinct from latent heat flux, and it is computed with respect to $0°C$ in the following manner:

$$\text{evaporation heat } (\text{W/m}^2) = Q_{\text{evap}}\, C_p\, T_{\text{evap}}, \tag{4.20}$$

where Q_{evap} is the evaporative mass flux in kg/(m^2 sec), C_p is the water heat capacity, and T_{evap} is the temperature of evaporating water in degrees Celsius, with T_{evap} generally equal to the ocean sea surface temperature.

For models employing a virtual salt flux, in which there is no mass transport of water across the ocean surface, the field temperature_flux_due_to_evaporation_expressed_as_heat_flux_out_of_sea_water is set to zero.

- temperature_flux_due_to_runoff_expressed_as_heat_flux_into_sea_water: This field measures the heat of runoff that enters the liquid ocean, with respect to $0°C$. This heat is computed as

$$\text{runoff heat } (\text{W/m}^2) = Q_{\text{runoff}}\, C_p\, T_{\text{runoff}}, \tag{4.21}$$

where Q_{runoff} is the liquid runoff mass flux in kg/(m^2 sec), C_p is the ocean heat capacity, and T_{runoff} is the temperature of liquid runoff in degrees Celsius. Note that this "runoff" mass flux may include melt from sea ice and melt from icebergs, in which case the name "runoff" is inappropriate, but is retained as a placeholder.

For models employing a virtual tracer flux, in which there is no mass transport of water across the ocean surface, the field temperature_flux_due_to_runoff_expressed_as_heat_flux_into_sea_water will be zero.

- heat_flux_into_sea_water_due_to_sea_ice_thermodynamics: This field accounts for heat gain by the liquid ocean when sea ice is formed, or heat loss from the liquid ocean when sea ice melts. It also includes the conductive heat flux from the ice-ocean interface into the sea ice. Note that the field upward_sea_ice_basal_heat_flux was asked for in CMIP3, and this field is closely related to the field asked for here. Whereas CMIP3 asked for the total heating of ice, in Watts, we ask for heating per horizontal area of ocean an ocean grid cell.

  The reason to bundle two heat fluxes together is that many ocean-ice models partition these terms in different manners. To expose some details, consider the discussion in Winton (2000), where we here consider heating of the liquid ocean to be positive. Equation (23) in Winton (2000) then reads

$$F_b = M_b - 4\,K\,(T_f - T_i)/h_i, \tag{4.22}$$

where F_b is the net heat flux into the liquid ocean associated with sea ice melt and formation, as well as conduction. The term $M_b > 0$ is the heat flux entering the liquid ocean during the formation of sea ice, whereas $M_b < 0$ is the heat flux lost from the liquid ocean upon melting sea ice. The second term on the right hand side is the conductive term, with K the thermal conductivity of sea ice. A value of $K = 2.03\,\text{W/(m °C)}$ is typical. T_f is the freezing temperature of seawater, with the ice-ocean interface assumed to be constantly at this temperature. T_i is the temperature of the sea ice. Finally, h_i is the sea ice thickness. The conductive term contributes a negative heat flux to the liquid ocean when the freezing temperature T_f is greater than the ice temperature T_i, and a positive heat flux for an oppositely signed temperature difference.

- heat_flux_into_sea_water_due_to_iceberg_thermodynamics: Icebergs transport calved land ice from the land into the ocean. A rudimentary "iceberg" model may simply be the insertion of calving land ice/snow into the ocean. More realistic iceberg models are being considered for climate modeling (Jongma et al., 2009). Melting of the icebergs into the liquid ocean is associated with a transfer of the latent heat of fusion from liquid ocean, and so represents a cooling of the liquid ocean in regions where the icebergs melt. It is this heat flux that is to be archived in the field heat_flux_into_sea_water_due_to_iceberg_thermodynamics.
- heat_flux_into_sea_water_due_to_snow_thermodynamics: Snow entering the liquid ocean is assumed to melt upon transferring its latent heat of fusion from the ocean. This cooling of the liquid ocean is what is to be archived in heat_flux_into_sea_water_due_to_snow_thermodynamics.
- surface_net_downward_longwave_flux: This field measures the net downward flux of longwave radiation that enters the liquid ocean.

- surface_downward_latent_heat_flux: This field measures the net flux of latent heating associated with the phase change from liquid ocean to water vapor.
- surface_downward_sensible_heat_flux: This field measures the net downward flux of sensible heating acting on the liquid ocean.
- surface_net_downward_shortwave_flux: This field measures the net downward flux of shortwave heating that hits the liquid ocean surface.
- downwelling_shortwave_flux_in_sea_water: This field measures the downwelling flux of shortwave heating within the three-dimensional liquid ocean. Shortwave radiation penetrates into the ocean column, with this penetration of fundamental importance for many ocean processes.
- heat_flux_correction: This field records the heat flux correction acting at the liquid ocean surface.

4.5.4 Boundary fluxes of momentum

- surface_downward_x_stress
- surface_downward_y_stress
- surface_downward_x_stress_correction
- surface_downward_y_stress_correction

These fluxes (Table 2.8) aim to present the analyst with sufficient information to quantify the net momentum imparted to the liquid ocean surface from the overlying atmosphere, sea ice, ice shelf, etc. Components of the vector stresses are aligned according to the ocean model's native grid, as these should be the flux components applied to the ocean model's surface grid cells.

4.6 In support of vertical/dianeutral SGS parameterizations

Thus far, we have recommended some fields that provide insight into the workings of various ocean subgrid scale (SGS) parameterizations. Table 2.9 presents additional fields to further characterize the parameterizations and their impact on the simulation, with focus on the vertical/dianeutral SGS parameterizations. In Section 4.6, we present fields helping to characterize lateral SGS parameterizations in the ocean models (see Table 2.10). In both cases, these fields are new relative to the CMIP3 fields discussed in WGCM (2007).

There is one limitation of the fields requested here that is worth highlighting. Although we recommend saving diffusivities and work terms, what is of more fundamental importance for characterizing the effects the SGS has on a field is the flux that it produces. Many fluxes are formulated as a diffusivity times a gradient. However, some parameterizations of fluxes are not expressed as such. Indeed, downgradient diffusion is not a good model for many SGS processes. It is for this reason that we ask for "buoyancy work from sgs parameterization" rather than just that from diffusivity. More generally, the protocols for saving fluxes rather than diffusivities and work need to be developed as more nontrivial SGS parameterizations become common.

We propose that dominant scientific use of the fields discussed in this subsection are realized by archiving *just* the climatological monthly means computed from 01JAN1986 to 31DEC2005 for the CMIP5 "historical" experiment. We thus recommend that only these fields be archived for CMIP5.

4.6.1 Vertical/dianeutral tracer diffusivities (2)

- ocean_vertical_heat_diffusivity
- ocean_vertical_salt_diffusivity
- ocean_vertical_tracer_diffusivity_due_to_background
- ocean_vertical_tracer_diffusivity_due_to_tides

Vertical/dianeutral tracer diffusivities used in modern IPCC class models typically consist of a static background value and a dynamically determined value. For the background diffusivity, some modelers choose a globally constant value, whereas others impose spatial dependence. There is evidence that the background diffusivity influences such processes as ENSO variability and overturning strength in model simulations. Hence, it is very important to have this field archived.

There are an increasingly large number of physical processes used by IPCC-class models that affect the vertical tracer diffusivity. For example, vigorous mixing processes in the upper ocean are associated with large mixing coefficients; more quiescent processes in the ocean pycnocline region lead to much smaller coefficients; and enhanced mixing near the ocean bottom generally increases the mixing coefficients. Ideally, the mixing coefficients corresponding to each of the separate processes will be archived.

It is difficult to anticipate the full suite of physical processes affecting the vertical/dianeutral diffusivity. As a start, we identify the following processes that are commonly found in IPCC class models, whose corresponding diffusivities would be of use in the CMIP5 archive:

- Static background tracer diffusivity meant to parameterize the background internal wave field;
- Tidal induced tracer diffusivity, with all relevant tidal constituents contributing to the mixing (e.g., Simmons et al., 2004; Lee et al., 2006);
- Boundary layer diffusivity meant to parameterize mixing at or near the ocean boundaries.
- Total vertical/dianeutral diffusivity for temperature and salinity associated with all physical processes, including the background diffusivity.

The background, tidal, and boundary layer diffusivities are the same for temperature, salinity, and other tracers. The total diffusivities may differ, however, if including a parameterization of double diffusive processes. In many implementations of boundary layer processes, the effects from double diffusion are wrapped into the boundary layer diffusivities. Hence, we write the diffusivities κ for temperature and salinity in the following form

$$\kappa^{\theta} = \kappa_{\text{back}} + \kappa_{\text{tides}} + \kappa^{\theta}_{\text{boundary+dd}} \tag{4.23}$$

$$\kappa^{S} = \kappa^{S}_{\text{back}} + \kappa_{\text{tides}} + \kappa^{S}_{\text{boundary+dd}} \tag{4.24}$$

We request archival of the following diffusivities

- κ^{θ}= ocean_vertical_heat_diffusivity
- κ^{S}= ocean_vertical_salt_diffusivity
- κ_{back}= ocean_vertical_tracer_diffusivity_due_to_background
- κ_{tides}= ocean_vertical_tracer_diffusivity_due_to_tides,

from which the boundary layer plus double diffusion diffusivities can be deduced.

4.6.2 Vertical/dianeutral momentum diffusivities (2)

- ocean_vertical_momentum_diffusivity
- ocean_vertical_momentum_diffusivity_due_to_background
- ocean_vertical_momentum_diffusivity_due_to_tides
- ocean_vertical_momentum_diffusivity_due_to_form_drag

As for tracers, the vertical/dianeutral diffusivities (also called kinematic viscosities) used in modern IPCC class models typically consist of a static background value and a dynamically determined value. The dynamically determined value is often determined as a function of the tracer diffusivity, with an assumed Prandtl number. In general, it is important to archive the viscosities in order to help characterize the parameterizations.

We write the total vertical/dianeutral momentum viscosity as the sum

$$\nu = \nu_{\text{back}} + \nu_{\text{form drag}} + \nu_{\text{boundary}} + \nu_{\text{tides}}. \tag{4.25}$$

These viscosities arise from the following processes:

- Static background vertical/dianeutral viscosity, meant to parameterize the background internal wave field;
- Vertical/dianeutral viscosity aimed at parameterizing mesoscale eddy induced form-drag (Greatbatch and Lamb, 1990; Ferreira and Marshall, 2006);
- Planetary boundary layer processes (e.g., Large et al., 1994);
- Tidal induced vertical/dianeutral viscosity (e.g., Simmons et al., 2004; Lee et al., 2006).

We request archival of the following momentum viscosities

- ν= ocean_vertical_momentum_diffusivity
- ν_{back}= ocean_vertical_momentum_diffusivity_due_to_background
- ν_{tides}= ocean_vertical_momentum_diffusivity_due_to_tides
- $\nu_{\text{form drag}}$= ocean_vertical_momentum_diffusivity_due_to_form_drag

from which the boundary layer diffusivities can be deduced.

4.6.3 Rate of work done against stratification (2)

- tendency_of_ocean_potential_energy_content
- tendency_of_ocean_potential_energy_content_due_to_tides
- tendency_of_ocean_potential_energy_content_due_to_background

A vertical/dianeutral diffusivity impacts the solution only in regions where there are nontrivial vertical tracer gradients. A measure of the impact can be deduced by mapping the rate at which work is done against the stratification by the tracer diffusivity. This work against stratification also impacts the potential energy budget, hence the name for the variables. We recommend mapping this work rate per horizontal area as a three-dimensional field.[28]

4.6.4 Frictional dissipation of kinetic energy by vertical viscosity (2)

- ocean_kinetic_energy_dissipation_per_unit_area_due_to_vertical_friction

Friction dissipates kinetic energy, especially in those regions of nontrivial shear. In characterizing the manner in which viscous friction affects the energy budget in an ocean model (Wunsch and Ferrari, 2004), it is important to map the energy dissipation.[29] It is sufficient for most purposes to map the dissipation from just the total vertical viscosity, rather than to partition it into separate processes.

4.7 In support of lateral SGS parameterizations

In this section, we present fields helping to characterize lateral SGS parameterizations in the ocean, with Table 2.10 summarizing the fields. As for the vertical/dianeutral SGS parameterizations, we propose that dominant scientific use of the fields discussed in this subsection are realized by archiving *just* the climatological monthly means computed from 01JAN1986 to 31DEC2005 for the CMIP5 "historical" experiment. We thus recommend that only these fields be archived for CMIP5.

4.7.1 Lateral tracer diffusivities (2)

- ocean_tracer_bolus_laplacian_diffusivity
- ocean_tracer_bolus_biharmonic_diffusivity
- ocean_tracer_epineutral_laplacian_diffusivity
- ocean_tracer_epineutral_biharmonic_diffusivity
- ocean_tracer_xy_laplacian_diffusivity
- ocean_tracer_xy_biharmonic_diffusivity

It is important to archive diffusivities used for neutral diffusion (Solomon, 1971; Redi, 1982) (laplacian and/or biharmonic), laplacian eddy-induced transport (Gent and McWilliams, 1990; Gent et al., 1995), and biharmonic eddy induced transport (Roberts and Marshall, 1998). In addition, some models employ an along-coordinate surface diffusion, either Laplacian or biharmonic, to stabilize the numerical instabilities inherent in certain implementations of rotated neutral diffusion (Griffies et al., 1998). We thus ask for the following diffusivities to be archived for CMIP5:

- ocean_tracer_bolus_laplacian_diffusivity = eddy induced transport diffusivity for a Laplacian operator;
- ocean_tracer_bolus_biharmonic_diffusivity = eddy induced transport diffusivity for a biharmonic operator;
- ocean_tracer_epineutral_laplacian_diffusivity = epineutral or isopycnal diffusivity for a Laplacian operator;
- ocean_tracer_epineutral_biharmonic_diffusivity = epineutral or isopycnal diffusivity for a biharmonic operator;

- ocean_tracer_xy_laplacian_diffusivity = along-coordinate diffusivity for a Laplacian operator;
- ocean_tracer_xy_biharmonic_diffusivity = along-coordinate diffusivity for a biharmonic operator.

Note that for isopyncal models, the distinction between epineutral and along-coordinate diffusivities is often blurred, though there is in general a distinction. Also note that the term "bolus" should be used synonymously with "eddy-induced", with the term bolus used for historical reasons.

4.7.2 Eddy kinetic energy source from Gent et al. (1995) (2)

- tendency_of_ocean_eddy_kinetic_energy_content_due_to_bolus_transport

An energetic analysis of the extraction of potential energy from the Gent and McWilliams (1990); Gent et al. (1995) scheme indicates that it affects an increase in the eddy kinetic energy (Aiki and Richards, 2008). The rate of eddy kinetic energy increase, per unit horizontal area is

$$\text{rate of eddy kinetic energy increase, per unit horizontal area, from GM } (\mathrm{W/m^2}) = (\rho \, \mathrm{d}z) \, \kappa \, (N \, S)^2. \tag{4.26}$$

In this expression, N is the buoyancy frequency, S is the magnitude of the neutral slope, κ is the diffusivity setting the overall strength of the parameterization, $\rho \, \mathrm{d}z$ is the grid cell mass per horizontal area, with $\mathrm{d}z$ the cell thickness. In a Boussinesq model, the *in situ* density factor should be set to the constant Boussinesq reference density ρ_o used by the model.

4.7.3 Lateral momentum viscosities (2)

- ocean_momentum_xy_laplacian_diffusivity
- ocean_momentum_xy_biharmonic_diffusivity

We do not make the distinction between various methods used to compute the lateral momentum viscosities. Hence, we only recommend the total fields be archived from the ocean models in CMIP5:

- ocean_momentum_xy_laplacian_diffusivity = total lateral momentum Laplacian diffusivity
- ocean_momentum_xy_biharmonic_diffusivity = total lateral momentum biharmonic diffusivity.

4.7.4 Frictional dissipation by lateral viscosity (2)

- ocean_kinetic_energy_dissipation_per_unit_area_due_to_xy_friction

As for the vertical/dianeutral viscosity, we recommend archiving the maps of energy dissipation induced by the total lateral viscous friction.[30]

Notes

[9] As noted on page 47 of Gill (1982), with the exception of only a small percentage of the ocean, density in the World Ocean varies by no more than 2% from $1035\,\mathrm{kg\ m^{-3}}$. Hence, $\rho_o = 1035\,\mathrm{kg\ m^{-3}}$ is a sensible choice for the reference density used in a Boussinesq ocean climate model. However, some models may use a different value. For example, early versions of the GFDL ocean model (Cox, 1984) set $\rho_o = 1000\,\mathrm{kg\ m^{-3}}$.

[10] In a mass conserving non-Boussinesq fluid, the total mass of liquid seawater, $\mathcal{M} = \sum_{i,j,k} \rho \, \mathrm{d}x \, \mathrm{d}y \, \mathrm{d}z$, evolves according to the budget

$$\partial_t \mathcal{M} = \sum_{i,j} \mathrm{d}x \, \mathrm{d}y \, Q^{\mathrm{w}}, \tag{4.27}$$

where ρ the *in situ* density, $\mathrm{d}x \, \mathrm{d}y$ the horizontal area of a grid cell, $\mathrm{d}z$ the vertical thickness (generally time dependent), and Q^{w} ($\mathrm{kg\ m^{-2}\ s^{-1}}$) is the net mass flux of water that crosses the liquid ocean boundaries, per horizontal cross-sectional area. Conservation of mass is a fundamental feature of a non-Boussinesq ocean which, unfortunately, is not respected by all non-Boussinesq models. Hence, it is useful to archive the total mass and boundary fluxes in order to quantify the level to which the model conserves.

[11] In a volume conserving Boussinesq fluid, the total volume of liquid seawater, $\mathcal{V}^{\mathrm{Bouss}} = \sum_{i,j,k} \mathrm{d}x \, \mathrm{d}y \, \mathrm{d}z$, evolves according to the budget

$$\partial_t \mathcal{V}^{\mathrm{Bouss}} = \sum_{i,j} \mathrm{d}x \, \mathrm{d}y \, Q^{\mathrm{w}} / \rho_o. \tag{4.28}$$

Conservation of volume is a fundamental feature of a Boussinesq ocean which, unfortunately, is not respected by all Boussinesq ocean models. Hence, it is useful to archive the volume and boundary flux fields to quantify the level to which the model conserves.

[12]The purpose of this endnote is to identify the differences in sea level reported from a Boussinesq model from that in a non-Boussinesq model. For this purpose, we note that mass conservation for a non-Boussinesq fluid column is given by

$$\partial_t \left(\int_{-H}^{\eta} \rho \, dz \right) = -\nabla \cdot \mathbf{U}^{\rho} + Q^{w}, \tag{4.29}$$

where η is the deviation of the sea surface from the $z = 0$ geopotential surface, $z = -H(x, y)$ is the ocean bottom,

$$\mathbf{U}^{\rho} = \int_{-H}^{\eta} \rho \, \mathbf{u} \, dz \tag{4.30}$$

is the vertically integrated mass transport, and Q^{w} the mass of seawater per time per horizontal area crossing the ocean boundaries. This equation says that the mass per area of a fluid column has a time tendency determined by the convergence of mass carried by ocean currents into the column (the $-\nabla \cdot \mathbf{U}^{\rho}$ term), plus boundary fluxes of mass (the Q^{w} term). We can extract from the mass budget (4.29) the following equation for the sea level

$$\partial_t \eta = \frac{-\nabla \cdot \mathbf{U}^{\rho} + Q^{w} - D \, \partial_t \overline{\rho}^{z}}{\overline{\rho}^{z}}, \tag{4.31}$$

where

$$\overline{\rho}^{z} = D^{-1} \int_{-H}^{\eta} \rho \, dz \tag{4.32}$$

is the vertically averaged density in a column of seawater, and $D = H + \eta$ the thickness of the seawater column from the ocean bottom to the ocean surface. There are three terms on the right hand side of equation (4.31) that affect the sea level evolution. The mass convergence arises from dynamical currents moving mass around in a fluid column; the boundary flux of mass is known as a *eustatic term*; and the term $-D \, \partial_t \overline{\rho}^{z}$ gives rise to an increase in sea surface height when the vertically averaged density reduces (e.g., as from warming or freshening), with this change is known as a *steric effect*. Note that these three terms are weighted by the inverse of the column averaged density, so that the surface height changes more in regions of low density.

For a Boussinesq fluid, the seawater density factors in equation (4.31) are set to the constant reference density ρ_o, in which case the Boussinesq surface height evolves according to

$$\partial_t \eta^{\text{Bouss}} = -\nabla \cdot \mathbf{U} + Q^{w} / \rho_o. \tag{4.33}$$

Notably, there are no direct changes to η^{Bouss} from changes in the column averaged density. Instead, changes in density only affect the Boussinesq sea level indirectly as manifest through changes in the ocean currents affecting $-\nabla \cdot \mathbf{U}$. Such limitations must be recognized when using the sea surface height in Boussinesq models as an approximation to the sea level. For example, as pointed out by Greatbatch (1994), a horizontally uniform change in column averaged density will induce no changes to the currents, and so it will not alter η^{Bouss}. However, η will change from the steric term.

[13]To understand the basics of how the global mean sea level changes, consider the following relation between the total mass of liquid seawater, total volume of seawater, and global mean seawater density,

$$\mathcal{M} = \mathcal{V} \, \overline{\rho}, \tag{4.34}$$

where $\mathcal{M}$ is the total liquid ocean mass (equation (4.1)), $\mathcal{V}$ is the total ocean volume (equation (4.3)), and $\overline{\rho}$ is the global mean *in situ* density

$$\overline{\rho} = \frac{\sum dx \, dy \, dz \, \rho}{\sum dx \, dy \, dz}. \tag{4.35}$$

Temporal changes in total ocean mass are affected by a nonzero net mass flux through the ocean boundaries (equation (4.27))

$$\partial_t \mathcal{M} = \mathcal{A} \, \overline{Q^{w}} \tag{4.36}$$

where $\overline{Q^{w}} = \mathcal{A}^{-1} \sum dx \, dy \, Q^{w}$ is the global mean mass per horizontal area per time of water crossing the ocean boundaries, with $\mathcal{A} = \sum dx \, dy$ the area of the global ocean surface. Temporal changes in the ocean volume are associated with sea level changes via

$$\partial_t \mathcal{V} = \mathcal{A} \, \partial_t \overline{\eta}, \tag{4.37}$$

where

$$\overline{\eta} = \mathcal{A}^{-1} \sum \eta \, dx \, dy \tag{4.38}$$

is the global mean sea level. Bringing these results together leads to the evolution equation for the mean sea level

$$\partial_t \overline{\eta} = \frac{\overline{Q^{w}}}{\overline{\rho}} - \left(\frac{\mathcal{V}}{\mathcal{A}} \right) \frac{\partial_t \overline{\rho}}{\overline{\rho}}. \tag{4.39}$$

The first term in equation (4.39) alters sea level by adding or subtracting mass from the ocean, with the name *eustatic* associated with these processes. The second term arises from temporal changes in the global mean density; i.e., from *steric* effects. The steric effect is

missing in Boussinesq models, so that the global mean sea level in a Boussinesq model is altered only by net volume fluxes across the ocean surface.

We can approximate each of the terms in equation (4.39) over a finite time Δt via

$$\Delta\overline{\eta} \approx \frac{\overline{Q^{w}}\,\Delta t}{\overline{\rho}} - \left(\frac{\mathcal{V}}{\mathcal{A}}\right)\frac{\Delta\overline{\rho}}{\overline{\rho}}, \tag{4.40}$$

where the Δ operator is a finite difference over the time step of interest. In a Boussinesq model, we must compute each term on the right hand side in order to develop an accurate time series for the global mean sea level that includes steric effects. For a non-Boussinesq model, $\overline{\eta}$ is computed directly from the model's surface height field, since the prognostic model includes steric effects.

In either the Boussinesq or non-Boussinesq case, it is of interest to diagnose the steric term

$$\mathcal{S} \equiv -\left(\frac{\mathcal{V}}{\mathcal{A}}\right)\frac{\Delta\overline{\rho}}{\overline{\rho}} \tag{4.41}$$

in order to deduce the effect on $\overline{\eta}$ associated just with changes in global mean density, as distinct from changes in ocean mass. The steric effect is straightforward to diagnose from a model simulation, given temporal changes in the global mean density.

For CMIP5, we are interested in the change in sea level in a global warming scenario experiment, with respect to a reference state defined by the initial conditions of the experiment. In this case, the steric term at a time n is given by

$$\begin{aligned}\mathcal{S} &= -\left(\frac{\mathcal{V}^{0}}{\mathcal{A}}\right)\frac{\overline{\rho^{n}} - \overline{\rho^{0}}}{\overline{\rho^{0}}} \\ &= \left(\frac{\mathcal{V}^{0}}{\mathcal{A}}\right)\left(1 - \frac{\overline{\rho}^{n}}{\overline{\rho^{0}}}\right),\end{aligned} \tag{4.42}$$

where $\rho^{0} = \rho(\theta^{0}, S^{0}, p^{0})$ is the *in situ* density for a grid cell as determined by the grid cell's reference temperature, salinity, and pressure, $\rho^{n} = \rho(\theta^{n}, S^{n}, p^{n})$ is the *in situ* density at time step n, and $\mathcal{V}^{0}$ is the reference volume of seawater.

[14]The time tendency for global mean density can be written as

$$\partial_{t}\overline{\rho} = \overline{\partial_{t}\,\rho} + \mathcal{V}^{-1}\iint \mathrm{d}x\,\mathrm{d}y\,(\rho(\eta) - \overline{\rho})\,\partial_{t}\,\eta, \tag{4.43}$$

where $\rho(\eta)$ is the density at the ocean surface. It is the first term in this equation that interests us when considering thermal effects, in which case we write

$$\overline{\partial_{t}\,\rho} = -\overline{\alpha\,\rho\,\partial_{t}\,\theta} + \overline{\beta\,\rho\,\partial_{t}\,S} + \overline{c_{s}^{-2}\,\partial_{t}\,p}, \tag{4.44}$$

where $\alpha = -\rho^{-1}\,\partial\rho/\partial\theta$ is the thermal expansion coefficient, $\beta = \rho^{-1}\,\partial\rho/\partial S$ is the haline contraction coefficient, and $c_{s}^{2} = \partial p/\partial\rho$ is the squared sound speed. Given this expansion of the density tendency, we identify the thermosteric contribution to sea level as the following finite increment

$$\mathcal{S}^{\text{thermo}} \equiv \left(\frac{\mathcal{V}}{\mathcal{A}}\right)\frac{\overline{\alpha\rho\,\Delta(\theta)}}{\overline{\rho}}. \tag{4.45}$$

As for the steric term given by equation (4.42), we identify a thermosteric term that is defined with respect to a reference state

$$\mathcal{S}^{\text{thermo}} = \left(\frac{\mathcal{V}^{0}}{\mathcal{A}}\right)\frac{\overline{\alpha^{\theta^{n}}\,\rho^{\theta^{n}}\,(\theta^{n} - \theta^{0})}}{\overline{\rho^{0}}}, \tag{4.46}$$

where $\alpha^{\theta^{n}} = \alpha(\theta^{n}, S^{0}, p^{0})$ is the thermal expansion coefficient as a function of the evolving temperature and the reference salinity and reference pressure; likewise, $\rho^{\theta^{n}} = \rho(\theta^{n}, S^{0}, p^{0})$. The reason to evolve the thermal expansion coefficient is that it is a strong function of the water mass properties. As the temperature of these water masses change under a changing climate, it is important to allow α to feel these changes. An alternative expression for the thermosteric term is motivated by the expression (4.42) for the steric term, so that we compute

$$\mathcal{S}^{\text{thermo}} = \left(\frac{\mathcal{V}^{0}}{\mathcal{A}}\right)\left(1 - \frac{\overline{\rho(\theta^{n}, S^{0}, p^{0})}}{\overline{\rho^{0}}}\right). \tag{4.47}$$

That is, the density in the numerator is computed as a function of the local temperature, with salinity and pressure held constant at their reference value.

[15]McDougall (2003) argues for the use of an alternative prognostic field called *conservative temperature*, which is the potential enthalpy divided by a reference heat capacity. Conservative temperature is indeed more conservative than potential temperature, and so provides a more solid foundation for prognosing heat movement in the ocean. However, for comparison to other models and to observational data, we still recommend that ocean components in CMIP5 archive their potential temperature field, whether the models consider this field as prognostic (most common situation) or diagnostic (as when conservative temperature is prognostic).

[16]According to the results of Griffies et al. (2009), one should *not* assume that all ocean models in CMIP5 are written with numerical methods that ensure the conservation of scalar fields such as mass, heat, and salt. One means to check for heat conservation is to compute the change in total heat over a specified time (say over a year), and compare that change to the total boundary heat input to the ocean system. The change in heat should agree to the heat input through the boundaries, with agreement to within numerical roundoff expected from a conservative model.

If there is a difference greater than numerical roundoff, then how significant is the difference? To answer this question, consider an order of magnitude calculation to determine the temperature trend that one may expect, given a nonzero net heat flux through the ocean boundaries. For simplicity, assume a Boussinesq fluid with constant volume (i.e., no net volume fluxes), so that the global mean liquid ocean temperature evolves according to

$$(\mathcal{V}\,\rho_o\,C_p)\,\partial_t\,\overline{\theta} = \mathcal{A}\,\overline{Q^{\mathrm{H}}} \tag{4.48}$$

where $\mathcal{V}$ is the liquid ocean volume, $\mathcal{A} = \sum \mathrm{d}x\,\mathrm{d}y$ is the surface area of the ocean, and $\overline{Q^{\mathrm{H}}} = \mathcal{A}^{-1} \sum Q^{\mathrm{H}}\,\mathrm{d}x\,\mathrm{d}y$ is the global average boundary heat flux. Typical values for the World Ocean yield $\mathcal{V}\,\rho_o\,C_p \approx 5.4 \times 10^{24}\,\mathrm{J}/^\circ C$ and $\mathcal{A} = 3.6 \times 10^{14}\,\mathrm{m}^2$, leading to the decadal scale temperature trend

$$\frac{\Delta\overline{\theta}}{\text{decade}} \approx 0.02\,\overline{Q^{\mathrm{H}}}. \tag{4.49}$$

For example, with a $1\,\mathrm{W\,m^{-2}}$ average heating of the ocean over the course of a decade (the net signal from global warming is on the order of $1\,\mathrm{W\,m^{-2}}$), we expect a global mean temperature trend of roughly $0.02^\circ C$ per decade, or $0.2^\circ C$ per century. If there is an error in the balance (4.48), we may define a global mean heat flux

$$Q^{\text{error}} \equiv \overline{Q^{\mathrm{H}}} - \mathcal{A}^{-1}\,(\mathcal{V}\,\rho_o\,C_p)\,\partial_t\,\overline{\theta}. \tag{4.50}$$

To translate the error in the net heating into an error in the temperature trend, use relation (4.49) to define

$$\frac{\Delta\overline{\theta}^{\text{error}}}{\text{decade}} \approx 0.02\,Q^{\text{error}}. \tag{4.51}$$

[17] As examples, note that CCSM plans to use 60 vertical levels for their ocean model in CMIP5, and GFDL will continue to use 50 levels in one of its coupled models, and 63 layers in another.

[18] Contrary to the notes in WGCM (2007), practical salinity, measured on the practical salinity scale, is *not* identical to absolute salinity, measured in $\mathrm{g\ kg^{-1}}$. Practical Salinity of a sample of seawater is derived from a measurment of its conductivity, while absolute salinity is the total mass of dissolved material per mass of solution. Section 5 of Jackett et al. (2006) provides a discussion of the differences, and Millero et al. (2008) present a new definition of Standard Seawater (seawater of a specified reference composition of dissolved material). The composition of seawater does vary around the World Ocean, so the relationship between practical salinity S and absolute salinity S_A is rather complicated. If we ignore these compositional variations, and take seawater to always be of reference composition, then absolute salinity S_A is identical to reference salinity S_R, which is related to practical salinity S according to

$$S_R(\mathrm{g/kg}) = (35.16504/35)(\mathrm{g/kg})\ S(\mathrm{psu}). \tag{4.52}$$

Hence, seawater of practical salinity $S = 35$ corresponds to an absolute salinity of $S_R = 35.16504\,\mathrm{g\ kg^{-1}}$. Due to the ongoing work of the SCOR/IAPSO Working Group 127, it is anticipated that by the year 2011, the oceanographic community will employ a standard measure of salinity based on absolute salinity rather than practical salinity. In the meantime, we recommend that ocean models continue to assume their salinity variable indeed measures practical salinity. The only (minor) issue that arises with this interpretation is that fresh water concentration of a seawater parcel should be computed as

$$FW = (1 - 10^{-3}\,S_A), \tag{4.53}$$

where again S_A is the absolute salinity. Assuming the absolute salinity is the same as the reference salinity, then

$$FW \approx (1 - 1.0047 \times 10^{-3}\,S), \tag{4.54}$$

where $35.16504/35 \approx 1.0047$.

[19] The density factor ρ in a non-Boussinesq fluid becomes the constant ρ_o for Boussinesq fluids.

[20] The kinematic balance (4.31) for a non-Boussinesq fluid leads to the nontrivial divergence

$$\nabla \cdot \mathbf{U}^\rho = -\partial_t\,(D\,\overline{\rho}) + Q^{\mathrm{w}}, \tag{4.55}$$

whereas for a Boussinesq fluid, equation (4.33) leads to the divergence

$$\nabla \cdot \mathbf{U} = -\eta_{,t}^{\mathrm{Bouss}} + Q^{\mathrm{w}}/\rho_o. \tag{4.56}$$

[21] We consider the function

$$\psi^U(x,y) = -\int_{y_o}^{y} \mathrm{d}y'\,U^\rho(x,y'), \tag{4.57}$$

where the southern limit y_o is at Antarctica. Note that all intermediate ranges of latitude bands are included, so there are no shadow regions that may otherwise be isolated due to land/sea arrangements. By definition, the y derivative $\psi^U(x,y)$ yields the $\hat{\mathbf{x}}$-transport $\partial_y\,\psi^U = U^\rho$, yet the x derivative does not yield the $\hat{\mathbf{y}}$-transport due to the divergent nature of the vertically integrated flow. A complement function

$$\psi^V(x,y) = \psi^U(x_o,y) + \int_{x_o}^{x} \mathrm{d}x'\,V^\rho(x',y), \tag{4.58}$$

yields $\partial_x\,\psi^V = V^\rho$. In the special case of a Boussinesq rigid lid model absent surface water fluxes, ψ^U and ψ^V reduce to the single rigid lid barotropic streamfunction. In the more general case, comparison of ψ^U and ψ^V in climate model simulations at GFDL reveal that after just a few years of spin-up, patterns for the monthly means of ψ^U and ψ^V are very similar. This result provides evidence

that much of the large-scale vertically integrated circulation is nearly non-divergent. In this case, either function ψ^U and ψ^V renders a useful map of the vertically integrated mass transport. Due to its simplicity, we recommend that ψ^U be archived.

[22]The mixed layer has near-zero gradients of $\theta, salinity$, and density, as well as tracers such as CFCs. So most techniques to estimate the MLD rely on either a threshold gradient or a threshold change in one of these quantities, normally in potential temperature θ or density (see, for example Lorbacher et al., 2006; De Boyer Montegut et al., 2004; Monterey and Levitus, 1997). Relying solely on θ has the advantage of good observational data coverage, but this approach neglects salinity stratification associated with barrier layers (see e.g., Sprintall and Tomczak, 1992). In contrast, relying solely on density overlooks density-compensating changes in $\theta - S$, exaggerating the mixed layer depth.

The method we recommend for purposes of ocean model comparisons is that from Levitus (1982). Here, the MLD is defined based on meeting a "sigma-t" criterion. This method has the advantage that it is readily employed in off-line mode, thus supporting the use of monthly mean model fields, analogous to Levitus (1982).

[23]Large-scale vertical velocity is largely immeasurable in the real ocean. Hence, there is no observational motivation to archive vertical velocity. In contrast, horizontal velocity is measurable, thus motivating it being part of the CMIP5 archives.

[24]WGCM (2007) recommend partitioning the poleward overturning streamfunction into the Atlantic, Pacific, and Indian Oceans. However, to separate the Indian and Pacific Oceans is not sensible, since there is no meridional boundary separating these basins. Instead, the Atlantic-Arctic, Indian-Pacific, and World Ocean are physically relevant, and thus are recommended here. We make the same recommendation for the partioning of $\hat{\mathbf{y}}$-ward tracer transport into basins.

[25]We choose not to recommend plotting overturning on the neutral density coordinate from McDougall and Jackett (2005) in order to facilitate direct comparison of the density overturning streamfunction between isopycnal models, which are based on σ_{2000}, and non-isopycnal models.

[26]For the Gent et al. (1995) volume transport streamfunction in a Boussinesq fluid, we have

$$\begin{aligned}
\Psi^{\text{gm}}(y,s,t) &= -\int_{x_a}^{x_b} \mathrm{d}x \int_{-H}^{z(s)} v^{\text{gm}}\, \mathrm{d}z \\
&= \int_{x_a}^{x_b} \mathrm{d}x \int_{-H}^{z(s)} \partial_z \left(\kappa_{\text{gm}}\, S^y\right) \mathrm{d}z \\
&= \int_{x_a}^{x_b} \mathrm{d}x\, \kappa_{\text{gm}}\, S^y(z(s)),
\end{aligned} \tag{4.59}$$

where $\kappa_{\text{gm}} > 0$ is the diffusivity, S^y is the $\hat{\mathbf{y}}$ neutral slope, and $\kappa_{\text{gm}}\, S^y$ vanishes at the ocean bottom. As for the streamfunction Ψ defined by equation (4.17), we recommend archiving Ψ^{gm} on both depth/pressure levels and isopycnal (σ_{2000}) levels.

[27]The mass transport leaving the $\hat{\mathbf{y}}$-ward face of a grid cell is written here by $\mathcal{V}\, \mathrm{d}x = v\, \rho\, \mathrm{d}z\, \mathrm{d}x$, and so $C\, \mathcal{V}\, \mathrm{d}x$ measures the mass per time of tracer leaving the $\hat{\mathbf{y}}$-ward face. We now consider a decomposition of this transport by defining the basin average transport and basin average tracer concentration as follows

$$[\mathcal{V}] = \frac{\sum_i \mathrm{d}x\, \mathcal{V}}{\sum_i \mathrm{d}x} \tag{4.60}$$

$$[C] = \frac{\sum_i \mathrm{d}x\, C}{\sum_i \mathrm{d}x}, \tag{4.61}$$

along with the deviations from basin average

$$\mathcal{V} = [\mathcal{V}] + \mathcal{V}^* \tag{4.62}$$

$$C = [C] + C^*. \tag{4.63}$$

The discrete i-sum extends over the basin or global domain of interest, so that $\sum_i \mathrm{d}x\, \mathcal{V}$ is the total $\hat{\mathbf{y}}$-ward transport of seawater at this band at a particular ocean model vertical level. The resulting $\hat{\mathbf{y}}$-ward tracer transport becomes

$$\mathcal{H}(y,t) = \sum_i \sum_k \mathrm{d}x\, \mathcal{V}\, C \tag{4.64}$$

$$= \sum_i \sum_k \mathrm{d}x\, \left([\mathcal{V}]\,[C] + \mathcal{V}^*\, C^*\right), \tag{4.65}$$

where the k sum extends over the vertical cells in a column.

It is common to identify three components:

$$\text{y_flux_advect} = \sum_i \sum_k \mathrm{d}x\, \mathcal{V}\, C \tag{4.66}$$

$$\text{y_flux_over} = \sum_i \sum_k \mathrm{d}x\, [\mathcal{V}]\,[C] \tag{4.67}$$

$$\text{y_flux_gyre} = \sum_i \sum_k \mathrm{d}x\, \mathcal{V}^*\, C^*, \tag{4.68}$$

with

$$\text{y_flux_gyre} = \text{y_flux_advect} - \text{y_flux_over}. \tag{4.69}$$

This identity follows very simply when the advective flux takes on the form of either first order upwind or second order centered differences. It becomes more involved when considering higher order, or flux limited, advection schemes. In these general cases, this result serves as a defintion of the gyre component, so that the advective flux is built from the advection scheme used in the ocean model.

[28]The non-negative rate of work done against stratification by vertical/dianeutral diffusion of density is given by

$$\mathcal{P} \equiv \int \mathrm{d}V\, \kappa_\mathrm{d}\, \rho\, N^2, \tag{4.70}$$

where N^2 is the squared buoyancy frequency and κ_d is the vertical/dianeutral diffusivity corresponding to a particular SGS process. It is useful to map the integrand per unit area for each grid cell, which yields the rate of work per horizontal area for a grid cell of thickness $\mathrm{d}z$

$$\text{rate of work against stratification per horizontal area performed by vertical diffusion}(\mathrm{W/m^2}) = \kappa_\mathrm{d}\, \rho\, N^2\, \mathrm{d}z. \tag{4.71}$$

In this way, vertical integrals can be computed offline merely by taking a vertical sum. If we instead mapped the field $\kappa_\mathrm{d}\, \rho\, N^2$, then integrated amounts would not be computable accurately for those cases where the grid cell thickness is time dependent. These units also provide a means for directly comparing the work done by diffusion against the heat fluxes crossing the ocean boundaries.

Equation (4.70) assumes the heat and salt diffusivities are the same, which is the case for tidal and background diffusivities. For the full heat, κ^θ_d, and salt, κ^S_d, diffusivities, including double diffusion, we compute

$$\begin{aligned} &\text{rate of work against stratification per horizontal area performed by vertical diffusion}(\mathrm{W/m^2}) \\ &= -g\, \mathrm{d}z \left(\kappa^\theta_\mathrm{d} \frac{\partial \rho}{\partial \theta} \frac{\partial \theta}{\partial z} + \kappa^S_\mathrm{d} \frac{\partial \rho}{\partial S} \frac{\partial S}{\partial z} \right). \end{aligned} \tag{4.72}$$

[29]The energy dissipated at a grid box in a hydrostatic model from vertical/dianeutral viscous friction is $(\rho\, \mathrm{d}V)\, \kappa\, (\partial_z \mathbf{u} \cdot \partial_z \mathbf{u})$, where κ is the viscosity, $(\rho\, \mathrm{d}V)$ is the mass of the cell, and $\mathbf{u} = (u, v)$ is the horizontal velocity. Just as for the work done against stratification, it is useful to map the non-positive dissipation per horizontal area in a grid cell of thickness $\mathrm{d}z$, as given by

$$\text{dissipation per horizontal area from vertical friction}(\mathrm{W/m^2}) = -\kappa\, (\partial_z \mathbf{u} \cdot \partial_z \mathbf{u})\, \rho\, \mathrm{d}z. \tag{4.73}$$

In this way, vertical integrals can be computed offline merely by taking a vertical sum.

[30]The local energy dissipated in a hydrostatic model by a lateral Laplacian friction with isotropic viscosity A and anisotropic viscosity D (see Section 17.8.2 of Griffies, 2004) is given by the non-positive quantity

$$\mathcal{D} = -(\rho\, \mathrm{d}V) \left[A\, (e_\mathrm{T}^2 + e_\mathrm{S}^2) + 2\, D\, \Delta^2 \right], \tag{4.74}$$

where $e_\mathrm{T} = (\mathrm{d}y)\, (u/\mathrm{d}y)_{,x} - (\mathrm{d}x)\, (v/\mathrm{d}x)_{,y}$ and $e_\mathrm{S} = (\mathrm{d}x)\, (u/\mathrm{d}x)_{,y} + (\mathrm{d}y)\, (v/\mathrm{d}y)_{,x}$ are the deformation rates, θ is an angle that sets the alignment of the generally anisotropic viscosity (Large et al., 2001; Smith and McWilliams, 2003), $2\,\Delta = e_\mathrm{S} \cos 2\theta - e_\mathrm{T} \sin 2\theta$, and $\mathrm{d}x$ and $\mathrm{d}y$ are the horizontal grid elements. We recommend archiving three-dimensional maps of the dissipation per horizontal area for a cell of thickness $\mathrm{d}z$

$$\text{dissipation per horizontal area from lateral laplacian friction}(\mathrm{W/m^2}) = -(\rho\, \mathrm{d}z) \left[A\, (e_\mathrm{T}^2 + e_\mathrm{S}^2) + 2\, D\, \Delta^2 \right]. \tag{4.75}$$

As defined, vertical integrals can be computed offline merely by taking a vertical sum.

The local energy dissipated in a hydrostatic model by a lateral biharmonic friction is given by the non-positive quantity (see Section 17.9.2 of Griffies, 2004)

$$\mathcal{D} = -(\rho\, \mathrm{d}V)\, \mathbf{F} \cdot \mathbf{F}, \tag{4.76}$$

where $\rho\, \mathrm{d}V\, \mathbf{F}$ is the lateral Laplacian friction vector used to build up the biharmonic operator. As for the dissipation from vertical viscosity, we recommend mapping the dissipation per horizontal area for each grid cell of thickness $\mathrm{d}z$, as given by

$$\text{dissipation per horizontal area from lateral biharmonic friction}(\mathrm{W/m^2}) = -(\rho\, \mathrm{d}z)\, \mathbf{F} \cdot \mathbf{F}. \tag{4.77}$$

Again, vertical integrals can be computed offline merely by taking a vertical sum.

Chapter 5

Concluding Comments

We hope that this document presents the climate science community with a useful reference to help finalize the ocean model protocols used in CMIP5. Some of the material here will be of use for modelers developing the diagnostic tools in anticipation of their CMIP5 simulations, and some material will assist analysts aiming to understand precisely what was saved.

We nonetheless recognize that this document is incomplete. For example, there are numerous further model fields that could be of use for ocean model comparison research, and thus for supporting the IPCC model assessment process. We could also present far more scientific discussion of certain fields, thus better motivating their archival. We are very happy to consider future recommendations of fields that have been omitted here, acknowledging that this report should be revised for future comparisons (e.g., CMIP6). In turn, there is some balance required between asking for too much and too little. Anticipating some criticism of asking for too much, we reemphasize those areas where output reduction has been employed by, for example, saving certain fields for only the historical experiment, and saving only the 20 year monthly climatologies of certain subgrid scale parameters (Section 1.3). Such output reduction methods allow for the newly requested fields to represent only a modest increase in overall archive requirements.

It is useful to highlight certain questions that remain unanswered by this document. Developing workable answers for these questions is somewhat time critical as model resolutions are refined, and the use of more complex horizontal and vertical grids becomes common.

- **Grid Standards and Remapping**: We presented a discussion of spatial sampling in Sections 1.1 and 3.1.2, at which point we highlighted the incomplete status of a generally agreed upon grid specification standard. The absence of a standard greatly handicaps the community-wide ability to address issues such as remapping. It is of fundamental importance that the community agree on a grid specification standard in the very near future.
- **Eddy statistics**: Ocean model resolutions of $1/4^\circ$ or finer are actively being considered by various groups for AR5, with future assessments likely to see even more models of this eddying class. In this document, we made no comment on the needs of sampling fields to develop robust eddy statistics, with much work required to prescribe general recommendations.[31]
- **3d Term Balances**: A mechanistic understanding of ocean processes typically requires the analysis of detailed budget terms, in addition to boundary forcing. For tracer budgets, one generally requires grid cell tendencies and flux components from advection and all SGS processes. For momentum budgets, one may require all the forces and transport processes acting to alter momentum. Beyond tracer and momentum, there are budgets for diagnostic fields that may be of interest, such as potential vorticity. In this document, we did not propose saving such detailed budget terms for CMIP5, both due to time limitations in preparing this document, and anticipated limits to the CMIP5 archive. However, more careful thought may arrive at a middle ground. Two approaches seem prudent: (A) a limited number of 3d budget terms be saved that allow for a nontrivial process analysis, even if incomplete; (B) a full suite of fluxes and forces are saved over a very limited *intense sampling* period.
- **SGS Parameterizations**: As mentioned in Section 4.6, many SGS parameterizations are not represented as downgradient diffusion. Protocols for saving fluxes rather than diffusivities need to be developed, especially as nontrivial SGS parameterizations become common.
- **Vertical Coordinates for Analysis**: There are many ocean science questions that are best addressed within the kinematic framework of a particular vertical coordinate. The commonly used geopotential/pressure option is just one choice. Hence, we must continue to ask questions concerning what vertical coordinate(s) provides the most

physical insight for a particular diagnostic field. Answers to these questions will likely lead to recommendations for how to sample certain fields from the models. Sampling on alternative coordinate surfaces is a likely outcome of the growing sophistication of the ocean model output used in CMIP.

Acknowledgements
We thank John Church and John Hunter for useful comments on early drafts of this document.

Bibliography

Adcroft, A. and Campin, J.-M.: Rescaled height coordinates for accurate representation of free-surface flows in ocean circulation models, Ocean Modelling, 7, 269–284, 2004.

Adcroft, A. and Hallberg, R. W.: On methods for solving the oceanic equations of motion in generalized vertical coordinates, Ocean Modelling, 11, 224–233, 2006.

Aiki, H. and Richards, K.: Energetics of the global ocean: the role of layer-thickness form drag, Journal of Physical Oceanography, 38, 1845–1869, 2008.

Bryan, F., Danabasoglu, G., Gent, P., and Lindsay, K.: Changes in ocean ventilation during the 21st century in the CCSM3, Ocean Modelling, 15, 141–156, 2006.

Bryan, K.: A numerical method for the study of the circulation of the world ocean, Journal of Computational Physics, 4, 347–376, 1969.

Campin, J.-M., Marshall, J., and Ferreira, D.: Sea ice-ocean coupling using a rescaled vertical coordinate z^*, Ocean Modelling, 24, 1–14, 2008.

Cotter, C. and Gorman, G.: Diagnostic tools for 3D unstructured oceanographic data, Ocean Modelling, 20, 170–182, 2008.

Cox, M. D.: A Primitive Equation, 3-Dimensional Model of the Ocean, NOAA/Geophysical Fluid Dynamics Laboratory, Princeton, USA, 1984.

Cunningham, S., Alderson, S., King, B., and Brandon, M.: Transport and variability of the Antarctic Circumpolar Current in Drake Passage, Journal of Geophysical Research, 108, Art. 8084, 2003.

De Boyer Montegut, C., Madec, G., Fischer, A., Lazar, A., and Iudicone, D.: Mixed layer depth over the global ocean: An examination of profile data and a profile based climatology, Journal of Geophysical Research, 109, doi:10.1029/2004JC002 378, 2004.

Delworth, T. L., Broccoli, A. J., Rosati, A., Stouffer, R. J., Balaji, V., Beesley, J. A., Cooke, W. F., Dixon, K. W., Dunne, J., Dunne, K. A., Durachta, J. W., Findell, K. L., Ginoux, P., Gnanadesikan, A., Gordon, C., Griffies, S. M., Gudgel, R., Harrison, M. J., Held, I. M., Hemler, R. S., Horowitz, L. W., Klein, S. A., Knutson, T. R., Kushner, P. J., Langenhorst, A. L., Lee, H.-C., Lin, S., Lu, L., Malyshev, S. L., Milly, P., Ramaswamy, V., Russell, J., Schwarzkopf, M. D., Shevliakova, E., Sirutis, J., Spelman, M., Stern, W. F., Winton, M., Wittenberg, A. T., Wyman, B., Zeng, F., and Zhang, R.: GFDL's CM2 Global Coupled Climate Models - Part 1: Formulation and Simulation Characteristics, Journal of Climate, 19, 643–674, 2006.

DeSzoeke, R. A. and Samelson, R. M.: The duality between the Boussinesq and Non-Boussinesq Hydrostatic Equations of Motion, Journal of Physical Oceanography, 32, 2194–2203, 2002.

Dukowicz, J. K., Smith, R. D., and Malone, R. C.: A reformulation and implementation of the Bryan-Cox-Semtner ocean model on the Connection Machine., Journal of Atmospheric and Oceanic Technology, 10, 195–208, 1993.

Dutay, J.-C., Bullister, J., Doney, S., Orr, J., Najjar, R., Caldeira, K., Campin, J.-M., Drange, H., Follows, M., Gao, Y., Gruber, N., Hecht, M., Ishida, A., Joos, F., Lindsay, K., Madec, G., Maier-Reimer, E., Marshall, J., Matear, R., Monfray, P., Mouchet, A., Plattner, G.-K., Sarmiento, J., Schlitzer, R., Slater, R., Totterdell, I., Weirig, M.-F., Yamanaka, Y.,

and Yool, A.: Evaluation of ocean model ventilation with CFC-11: comparison of 13 global ocean models, Ocean Modelling, 4, 89–120, 2002.

England, M. H.: The age of water and ventilation timescales in a global ocean model, Journal of Physical Oceanography, 25, 2756–2777, 1995.

Ferreira, D. and Marshall, J.: Formulation and implementation of a residual-mean ocean circulation model, Ocean Modelling, 13, 86–107, 2006.

Fissel, D., Birch, J., Melling, H., and Lake, R.: Non-tidal flows in the Northwest Passage, in Canadian Technical Report of Hydrography and Ocean Sciences, p. 142pp, Institute of Ocean Sciences, Sidney, Canada, 1998.

Fox-Kemper, B., Ferrari, R., and Hallberg, R.: Parameterization of mixed layer eddies. I: Theory and diagnosis, Journal of Physical Oceanography, in press, 2008.

Gent, P. R. and McWilliams, J. C.: Isopycnal mixing in ocean circulation models, Journal of Physical Oceanography, 20, 150–155, 1990.

Gent, P. R., Willebrand, J., McDougall, T. J., and McWilliams, J. C.: Parameterizing eddy-induced tracer transports in ocean circulation models, Journal of Physical Oceanography, 25, 463–474, 1995.

Gill, A.: Atmosphere-Ocean Dynamics, vol. 30 of International Geophysics Series, Academic Press, London, 662 + xv pp, 1982.

Gnanadesikan, A., Russell, J., and Zeng, F.: How does ocean ventilation change under global warming?, Ocean Science, 3, 43–53, 2007.

Gordon, A., Susanto, R., and Vranes, K.: Cool Indonesian throughflow as a consequence of restricted surface layer flow, Nature, 425, 824–828, 2003.

Greatbatch, R. J.: A note on the representation of steric sea level in models that conserve volume rather than mass., Journal of Geophysical Research, 99, 12 767–12 771, 1994.

Greatbatch, R. J. and Lamb, K. G.: On parameterizing vertical mixing of momentum in non-eddy resolving ocean models, Journal of Physical Oceanography, 20, 1634–1637, 1990.

Gregory, J., Church, J., Boer, G., Dixon, K., Flato, G., Jackett, D., Lowe, J., O'Farrell, S., Roeckner, E., Russell, G., Stouffer, R., and Winton, M.: Comparison of results from several AOGCMs for global and regional sea-level change 1900–2100, Climate Dynamics, 18, 225–240, 2001.

Griffies, S. M.: The Gent-McWilliams skew-flux, Journal of Physical Oceanography, 28, 831–841, 1998.

Griffies, S. M.: Fundamentals of ocean climate models, Princeton University Press, Princeton, USA, 518+xxxiv pages, 2004.

Griffies, S. M., Gnanadesikan, A., Pacanowski, R. C., Larichev, V., Dukowicz, J. K., and Smith, R. D.: Isoneutral diffusion in a z-coordinate ocean model, Journal of Physical Oceanography, 28, 805–830, 1998.

Griffies, S. M., Pacanowski, R., Schmidt, M., and Balaji, V.: Tracer Conservation with an Explicit Free Surface Method for z-coordinate Ocean Models, Monthly Weather Review, 129, 1081–1098, 2001.

Griffies, S. M., Gnanadesikan, A., Dixon, K. W., Dunne, J. P., Gerdes, R., Harrison, M. J., Rosati, A., Russell, J., Samuels, B. L., Spelman, M. J., Winton, M., and Zhang, R.: Formulation of an ocean model for global climate simulations, Ocean Science, 1, 45–79, 2005.

Griffies, S. M., Biastoch, A., Böning, C., Bryan, F., Chassignet, E., England, M., Gerdes, R., Haak, H., Hallberg, R. W., Hazeleger, W., Jungclaus, J., Large, W. G., Madec, G., Samuels, B. L., Scheinert, M., Gupta, A. S., Severijns, C. A., Simmons, H. L., Treguier, A. M., Winton, M., Yeager, S., and Yin, J.: Coordinated Ocean-ice Reference Experiments (COREs), Ocean Modelling, 26, 1–46, 2009.

Huang, R. X.: Real freshwater flux as a natural boundary condition for the salinity balance and thermohaline circulation forced by evaporation and precipitation, Journal of Physical Oceanography, 23, 2428–2446, 1993.

Huang, R. X., Jin, X., and Zhang, X.: An oceanic general circulation model in pressure coordinates, Advances in Atmospheric Physics, 18, 1–22, 2001.

Jackett, D. R., McDougall, T. J., Feistel, R., Wright, D. G., and Griffies, S. M.: Algorithms for density, potential temperature, conservative temperature, and freezing temperature of seawater, Journal of Atmospheric and Oceanic Technology, 23, 1709–1728, 2006.

Jongma, J., Driesschaert, E., Fichefet, T., Goosse, H., and Renssen, H.: The effect of dynamic-thermodynamic icebergs on the Southern Ocean climate in a three-dimensional model, Ocean Modelling, 26, 104–113, 2009.

Key, R., Kozyr, A., Sabine, C., Lee, K., Wanninkhof, R., Bullister, J., Feely, R., Millero, F., Mordy, C., and Peng, T.-H.: A global ocean carbon climatology: results from GLODAP, Global Biogeochemical Cycles, 18, GB4031, 2004.

Komori, N., Ohfuchi, W., Taguchi, B., Sasaki, H., and Klein, P.: Deep ocean inertia-gravity waves simulated in a high-resolution global coupled atmosphereocean GCM, Geophysical Research Letters, 35-L04610, 2008.

Large, W. G., McWilliams, J. C., and Doney, S. C.: Oceanic vertical mixing: A review and a model with a nonlocal boundary layer parameterization, Reviews of Geophysics, 32, 363–403, 1994.

Large, W. G., Danabasoglu, G., McWilliams, J. C., Gent, P. R., and Bryan, F. O.: Equatorial circulation of a global ocean climate model with anisotropic horizontal viscosity, Journal of Physical Oceanography, 31, 518–536, 2001.

Leaman, K., Molinari, R., and Vertes, P.: Structure and variability of the Florida Current at 27N: April 1982-July 1984, Journal of Physical Oceanography, 17, 565–583, 1987.

Lee, H.-C., Rosati, A., and Spelman, M.: Barotropic tidal mixing effects in a coupled climate model: Oceanic conditions in the northern Atlantic, Ocean Modelling, 3-4, 464–477, 2006.

Levitus, S.: Climatological atlas of the world ocean, U.S. Government Printing Office 13, NOAA, Washington, D.C., 163 pp., 1982.

Lorbacher, K., Dommenget, D., Niiler, P., and Köhl, A.: Ocean mixed layer depth: A subsurface proxy of ocean-atmosphere variability, Journal of Geophysical Research, 111-C07010, doi:10.1029/2003JC002 157, 2006.

Lukas, R. and Firing, E.: The geostrophic balance of the Pacific equatorial undercurrent, Deep-Sea Research, 31, 61–66, 1984.

Marshall, J., Adcroft, A., Campin, J.-M., Hill, C., and White, A.: Atmosphere-Ocean modeling exploiting fluid isomorphisms, Monthly Weather Review, 132, 2882–2894, 2004.

McAvaney, B., Covey, C., Joussaume, S., Kattsov, V., Kitoh, A., Ogana, W., Pitman, A. J., Weaver, A. J., Wood, R. A., Zhao, Z.-C., AchutaRao, K., Arking, A., Barnston, A., Betts, R., Bitz, C., Boer, G., Braconnot, P., Broccoli, A., Bryan, F., Claussen, M., Colman, R., Delecluse, P., Genio, A. D., Dixon, K., Duffy, P., Dmenil, L., England, M., Fichefet, T., Flato, G., Fyfe, J. C., Gedney, N., Gent, P., Genthon, C., Gregory, J., Guilyardi, E., Harrison, S., Hasegawa, N., Holland, G., Holland, M., Jia, Y., Jones, P. D., Kageyama, N., Keith, D., Kodera, K., Kutzbach, J., Lambert, S., Legutke, S., Madec, G., Maeda, S., Mann, M. E., Meehl, G., Mokhov, I., Motoi, T., Phillips, T., Polcher, J., Potter, G. L., Pope, V., Prentice, C., Roff, G., Semazzi, F., Sellers, P., Stensrud, D. J., Stockdale, T., Stouffer, R., Taylor, K. E., Trenberth, K., Tol, R., Walsh, J., Wild, M., Williamson, D., Xie, S.-P., Zhang, X.-H., , and Zwiers, F.: Model Evaluation, in Climate Change 2001: The Scientific Basis. Contribution of Working Group I to the Third Assessment Report of the Intergovernmental Panel on Climate Change, pp. 472–523, Cambridge University Press, Cambridge, UK, 2001.

McDougall, T. and Jackett, D.: The material derivative of neutral density, Journal of Marine Research, 63, 159–185, 2005.

McDougall, T. J.: Potential enthalpy: a conservative oceanic variable for evaluating heat content and heat fluxes., Journal of Physical Oceanography, 33, 945–963, 2003.

Melling, H.: Exchanges of freshwater through the shallow straits of the North American Arctic, in The freshwater budget of the Arctic Ocean, pp. 472–523, Kluwer Academic Publisher, 2000.

Mellor, G. L. and Yamada, T.: Development of a turbulent closure model for geophysical fluid problems, Reviews of Geophysics, 20, 851–875, 1982.

MERCATOR: List of internal metrics for the MERSEA-GODAE Global Ocean: Specification for implementation, in Integrated System Design and Assessment, France, 2006.

Millero, F., Feistel, R., Wright, D., and McDougall, T.: The composition of Standard Seawater and the definition of the Reference-Composition salinity scale, Deep-Sea Research, 55, 50–72, 2008.

Monterey, G. and Levitus, S.: Climatological cycle of mixed layer depth in the world ocean, U.S. government printing office, NOAA NESDIS, Washington, D.C., 5 pp., 1997.

Olsen, S., Hansen, B., Quadfasel, D., and Osterhus, S.: Observed and modelled stability of overflow across the Greenland-Scotland ridge, Nature, 455, doi:10.1038/nature07 302, 2008.

Osterhus, S., Turrell, W., Jonsson, S., and Hansen, B.: Measured volume, heat, and salt fluxes from the Atlantic to the Arctic Mediterranean, Geophysical Research Letters, 32, doi:10.1029/2004GL022 188, 2005.

Otto, L., Zimmerman, J., Furnes, G., Mork, M., Saetre, R., and Becker, G.: Review of the physical oceanography of the North Sea, Netherlands Journal of Sea Research, 26, 161–238, 1990.

Pinardi, N., Rosati, A., and Pacanowski, R. C.: The sea surface pressure formulation of rigid lid models. Implications for altimetric data assimilation studies, Journal of Marine Systems, 6, 109–119, 1995.

Redi, M. H.: Oceanic isopycnal mixing by coordinate rotation., Journal of Physical Oceanography, 12, 1154–1158, 1982.

Roach, A., Aagard, K., Pease, C., Salo, S., Weingartner, T., Pavlov, V., and Kulakov, M.: Direct measurements of transport and water properties through Bering Strait, Journal of Geophysical Research, 100, 18 443–18 457, 1995.

Roberts, M. J. and Marshall, D.: Do we require adiabatic dissipation schemes in eddy-resolving ocean models?, Journal of Physical Oceanography, 28, 2050–2063, 1998.

Russell, J., Dixon, K., Gnanadesikan, A., Stouffer, R., and Toggweiler, J.: Southern Ocean Westerlies in a warming world: Propping open the door to the deep ocean, Journal of Climate, 19, 6381–6390, 2006.

Sadler, H.: Water, heat and salt transports through Nares Strait, Ellesmere Island, Fisheries Research Board of Canada, 33, 22862295, 1976.

Schauer, U., Fahrbach, E., Osterhus, S., and Rohardt, G.: Arctic warming through the Fram Strait: Oceanic heat transport from 3 years of measurements, Journal of Geophysical Research, 109, doi:10.1029/2003JC001 823, 2004.

Sidorenko, D., Danilov, S., Wang, Q., Huerta-Casas, A., and Schröter, J.: On computing transports in nite-element models, Ocean Modelling, in press, 2008.

Simmons, H. L., Jayne, S. R., Laurent, L. C. S., and Weaver, A. J.: Tidally driven mixing in a numerical model of the ocean general circulation, Ocean Modelling, 6, 245–263, 2004.

Sloyan, B., Johnson, G., and Kessler, W.: The Pacific Cold Tongue: A pathway for interhemispheric exchange, Journal of Physical Oceanography, 33, 1027–1043, 2003.

Smith, R. and Gent, P.: Reference Manual for the Parallel Ocean Program (POP), Los Alamos Technical Report No. LAUR-02-2484, 2004.

Smith, R. D. and McWilliams, J. C.: Anisotropic horizonal viscosity for ocean models, Ocean Modelling, 5, 129–156, 2003.

Solomon, H.: On the representation of isentropic mixing in ocean models, Journal of Physical Oceanography, 1, 233–234, 1971.

Sprintall, J. and Tomczak, M.: Evidence of the Barrier Layer in the Surface Layer of the Tropics, Journal of Geophysical Research, 97, 7305–7316, 1992.

Stacey, M. W., Pond, S., and Nowak, Z. P.: A Numerical Model of the Circulation in Knight Inlet, British Columbia, Canada, Journal of Physical Oceanography, 25, 1037–1062, 1995.

Strong, A., Liu, G., Meyer, J., Hendee, J., and Sasko, D.: Coral Reef Watch 2002, Bulletin of Marine Science, 75, 259–268, 2004.

Thiele, G. and Sarmiento, J. L.: Tracer dating and ocean ventilation, Journal of Geophysical Research, 95, 9377–9391, 1990.

WGCM: IPCC Standard Output from Coupled Ocean-Atmosphere GCMs, CLIVAR WGCM Document, available from `http://www-pcmdi.llnl.gov/ipcc/standard_output.html`, 2007.

Winton, M.: A reformulated three-layer sea ice model, Journal of Atmospheric and Oceanic Technology, 17, 525–531, 2000.

Wunsch, C. and Ferrari, R.: Vertical Mixing, Energy, and the General Circulation of the Ocean, Annual Reviews of Fluid Mechanics, 36, 281–314, 2004.

Wunsch, C. and Stammer, D.: Satellite altimetry, the marine geoid, and the oceanic general circulation, Annual Reviews of Earth Planetary Science, 26, 219–253, 1998.

Yaremchuk, M., McCreary, J., Yu, Z., and Furue, R.: The South China Sea throughow retrieved from climatological data, Journal of Physical Oceanography, in press, 2008.

National Oceanography Centre, Southampton
University of Southampton Waterfront Campus
European Way, Southampton SO14 3ZH
United Kingdom
Tel: +44 (0) 23 8059 6777
Fax: +44 (0) 23 8059 6204
Email: icpo@noc.soton.ac.uk